Consequences of disease-causing small heat shock protein mutations on ARE-mediated mRNA decay

Senior Honors Thesis

By

Nicole Naiman

Undergraduate Biomedical Science Major

School of Allied Medical Professions

The Ohio State University

2011

Choose an item. Committee:

Dr. Stephen Kolb, M.D., Ph.D, Advisor

Dr. Daniel Battle, Ph.D.

Dr. Margaret Teaford, Ph.D.

Abstract

Motor neuron diseases (MNDs) are neurodegenerative diseases that involve loss of motor neurons in the brain and spinal cord. MNDs are debilitating and often fatal. Distal hereditary motor neuropathies (dHMNs) are a category of MND characterized by progressive, distal weakness without loss of sensation. The primary focus of our laboratory is to understand the functional consequences of mutations in small heat shock proteins (sHSPs) that result in dHMN. sHSPs comprise a family of 10 homologous proteins that are characterized by a central alpha-crystallin domain, are expressed ubiquitously, serve neuroprotective functions, and are upregulated by cell stress. To date, mutations in three sHSPs: HSPB1, HSPB3 and HSPB8, have been associated with dHMN. These mutations include HSPB1(R136W) and HSPB3(R7S). We propose that mutations reported in these proteins affect the same cellular pathway because they all lead to the same clinical phenotype and loss of motor neurons.

HSPB1 is the best characterized sHSP and is required for AU-rich element (ARE)-dependent mRNA decay. AREs are adenosine and uridine rich regions that are present in the 3' untranslated region of a subset of mRNAs that signal for their rapid decay. We hypothesize that dHMN-associated mutations result in dysregulation of this critical mRNA decay pathway, and that mutations in HSPB1 and in HSPB3 result in an increased half-life of ARE-containing mRNAs. To determine the effect of sHSP

mutations on ARE-mediated mRNA decay, we measured the rate of ARE-mediated mRNA decay in macrophages transfected with the wild-type HSPB1 gene or the mutant HSPB1(R136W) gene. However, these experiments must be replicated before conclusions can be drawn about the role of HSPB1(R136W) in ARE-mediated mRNA decay *in vitro*. To determine the effect of the HSPB1(R136W) on ARE-mediated mRNA decay *in vivo*, we developed transgenic mice expressing either the wild-type HSPB1 or mutant HSPB1(R136W) trangenes under the prion-protein promoter (PrP) to ensure high expression of the wild-type HSPB1 and mutant HSPB1(R136W) transgenes in neurons. We determined that expression of the PrP-driven HSPB1(R136W) transgene resulted in a subclinical motor neuropathy. We will use this mouse model in the future to determine the effect of mutant HSPB1(R136W) on ARE-mediated mRNA decay *in vivo*.

Little is known about the function of wild-type HSPB3 or about the effect of HSPB3(R7S) on that function. Therefore, we have begun to characterize wild-type and mutant HSPB3. Further studies must be performed to determine the effect of HSPB3 and HSPB3(R7S) on ARE-mediated mRNA decay *in vitro* and *in vivo*. Determining the effect of these small heat shock protein mutations on ARE-mediated mRNA decay *in vitro* and *in vivo* will further our mechanistic understanding of how small heat shock protein mutations lead to dHMN, and MNDs in general.

Acknowledgments

I would like to thank Dr. Stephen Kolb, Dr. Amit Srivastava, Dr. Shuping Gu and Samantha Renusch for all of their help and guidance with this research project. I would also like to thank the Dr. Phillip Popovich and his lab, Dr. Jill Raphael Fortney and her lab, Dr. Dana McTigue and her lab, as well as Dr. Glenn Lin and his lab for collaborating with us, and all of their help in conducting these experiments.

Thank you very much to Lori Martensen and Dr. Bruce Biagi for all of their guidance, support, and help during my undergraduate career.

Vita

August 2003 to June 2007..... Olmsted Falls High School

September 2007 to present..... The Ohio State University

Fields of Study

Major Field: Biomedical Science in the School of Allied Medical Professions

Table of Contents

List of Tables

List of Figures

Chapter 1

Problem Statement

Motor Neuron Diseases

Motor neuron diseases (MNDs) are neurodegenerative diseases characterized by motor neuron loss and progressive muscle weakness in the limbs. MNDs are debilitating, lead to poor quality of life, and are often fatal. Some examples of MNDs are amyotrophic lateral sclerosis (ALS), also known as Lou Gehrig's disease, the spinal muscular atrophies (SMAs), and the distal hereditary motor neuropathies (dHMNs). ALS is always fatal, but SMAs and dHMN are not necessarily fatal. In particular, about 6 in 100,000 people are diagnosed with ALS [1] and this disease is usually fatal within 5 years of the diagnosis [2]. Unfortunately, there are no effective treatments for MNDs. One of the interesting questions in MND research has to do with motor neuron selectivity: how do mutations in genes that are expressed in all cells result in a motor neuron selective disease?

To answer this question, the mechanism of MNDs must be determined. Because MNDs are related and have similar clinical phenotypes, MNDs may develop via a common mechanism that affects a common pathway. One of these proposed common pathways is altered RNA processing [3]. Altered ARE-mediated mRNA decay is hypothesized to contribute to the mechanism of dHMN (preliminary evidence).

Therefore, we studied ARE-mediated mRNA decay in different MND model systems to determine if altered ARE-mediated mRNA decay should be considered a possibility for a common affected pathway in MNDs. We hypothesize that ARE-mediated mRNA decay is altered in dHMN as well as other MNDs, including ALS.

Literature Review

Distal Hereditary Motor Neuropathy

Our laboratory primarily focuses on distal hereditary motor neuropathy (dHMN). dHMN is a debilitating MND characterized by progressive weakness in the toes and feet without loss of sensation [4]. In humans, there are axonal dHMNs and demylinating dHMNs. Certain mutations in small heat shock proteins have been associated with axonal dHMN [5-9].

Small Heat Shock Proteins

Small heat shock proteins (sHSPs) are a family of 10 homologous proteins characterized by a central alpha-crystallin domain responsible for the formation of sHSP complexes.[10,11]. sHSPs are expressed in all cells, and their expression is induced by a variety of cell stressors such as heat, ultraviolet light, and cardiac ischemia.[12,13]. Multiple functions have been ascribed to these proteins. Functions characterized thus far include the prevention of apoptosis, rearrangements of the cytoskeleton, their roles as molecular chaperones, and actin polymerization [10, 14].

Interestingly, mutations in 3 of these 10 proteins, HSPB1, HSPB3, and HSPB8, result in dHMN [5-7, 9] (Figure 1). These mutations include HSPB1(R136W) and HSPB3(R7S) [7, 9]. The overall goal of my research is to characterize the functional consequences of these mutations. The dHMN-associated sHSP mutations are not specific to any one sHSP domain (Figure 1). sHSP mutations associated with dHMN are found in the alpha-crystallin domain, the C-terminal domain, and the N-terminal domain. If all of these mutations occurred in the alpha-crystallin domain, then sHSP binding and complex formation would most likely contribute to the mechanism of these mutations leading to dHMN. However, only 2/3 of these sHSP disease-causing mutations occur in the alpha-crystallin domain. Therefore, there is most likely some other essential function of sHSPs that must be altered for dHMN to develop.

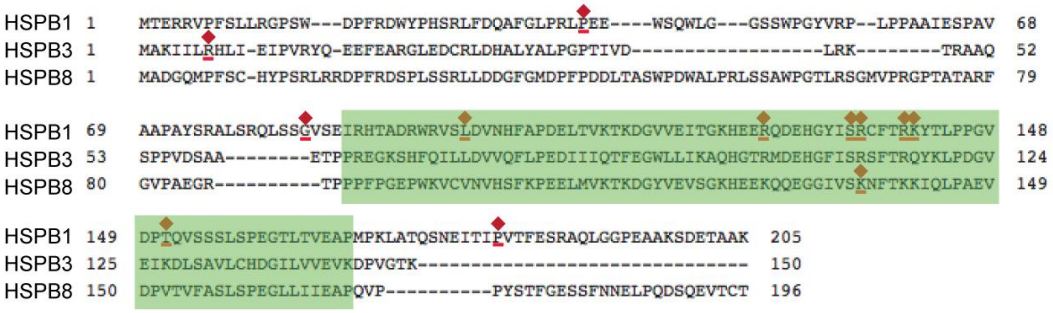

Figure 1. Mutations in sHSPs associated with dHMN.

Mutations in HSPB1, HSPB3, and HSPB8 that are associated with dHMN are indicated by the red diamonds. The green region denotes the alpha-crystallin domain.

Of the ten sHSPs, HSPB1 has been the most extensively studied. As discussed above, mutant HSPB1(R136W) causes dHMN [7]. However, wild-type HSPB1 is

actually neuroprotective in neurons, meaning that it promotes neuron survival [15]. Just as the mechanism of sHSP mutations causing dHMN is unknown, the mechanism by which wild-type HSPB1 is neuroprotective is also not known.

ARE-mediated mRNA decay

One important way that gene expression is controlled is by the regulation of mRNA decay. There are many different pathways involved in the decay of mRNAs. One of these pathways is ARE-mediated mRNA decay. AREs are adenosine and uridine rich regions in the 3' untranslated region of a subset of mRNAs [14]. It is known that when a protein complex called AUF1-and signal transduction regulated complex binds to an ARE, the complex attracts mRNA degradation machinery and initiates mRNA decay [14]. HSPB1 is part of this AUF1 protein complex that binds to the ARE and thus helps to initiate ARE-mediated mRNA decay (Figure 2) [14]. HSPB1 can only initiate mRNA decay if there is an ARE on an mRNA; otherwise, the AUF1 complex containing HSPB1 cannot bind to the mRNA, and the mRNA must be degraded via another mechanism, or it will not be degraded at all.

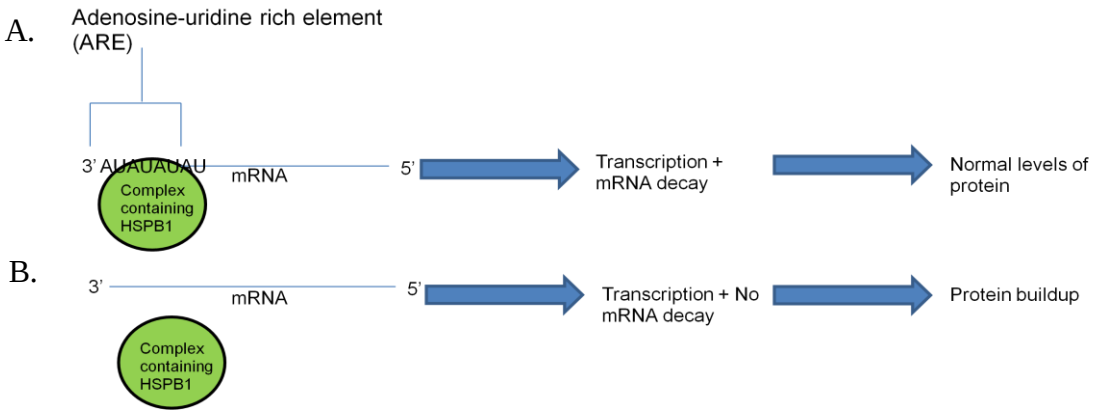

Figure 2. HSPB1 initiates ARE-mediated mRNA decay.

A. HSPB1 initiates ARE-mediated mRNA decay by binding to the ARE as part of the AUF1 complex. Normal levels of the transcribed protein are expressed.
B. HSPB1 does not initiate mRNA decay without an ARE. The transcribed protein is over-expressed.

We have hypothesized that ARE-mediated mRNA decay is altered in dHMN patients with HSPB1 mutations. To test this hypothesis, we developed a luciferase reporter assay. We transfected stable HeLa cells over-expressing wild-type or mutant HSPB1 with a wild-type or mutant luciferase reporter (Figure 3). The wild-type luciferase reporter did not have an ARE on its mRNA. The mutant luciferase reporter had the ARE region from TNFα on its mRNA. In the presence of wild-type HSPB1, the steady state level of the ARE luciferase reporter was decreased compared to the wild-type luciferase reporter. However, in the presence of HSPB1(R136W), the steady state level of the ARE luciferase reporter was the same as the steady state level of the wild-type luciferase reporter. This assay did not directly measure the rate of ARE-mediated mRNA decay; therefore, the observed increase in steady state levels of the ARE luciferase reporter in the presence of HSPB1(R136W) compared to in the presence of wild-type

HSPB1 could be a result of altered ARE-mediated mRNA decay of the ARE reporter, or a result of an increase in production of the ARE luciferase reporter in the presence of HSPB1(R136W). Currently, we are using assays that measure mRNA decay directly to clarify whether or not HSPB1(R136W) actually alters ARE-mediated mRNA decay.

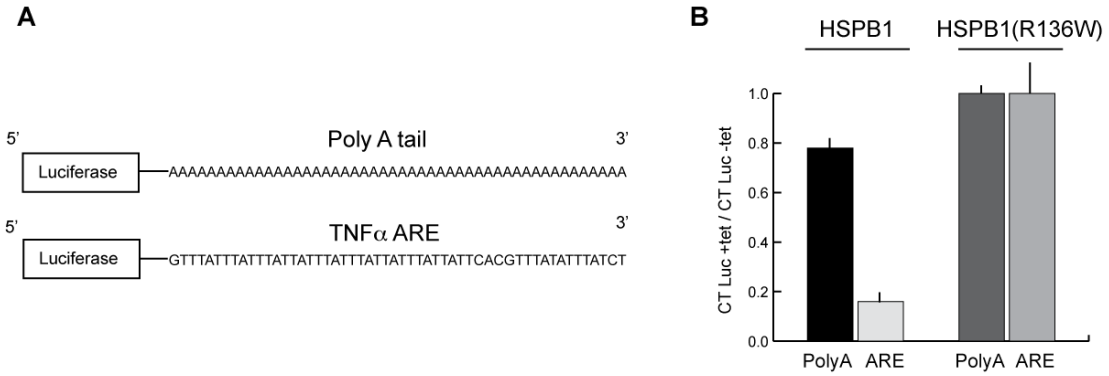

Figure 3. Preliminary evidence that HSPB1(R136W) inhibits ARE-mediated mRNA decay.

A. Constructs of the luciferase reporter genes. The wild-type luciferase reporter does not contain an ARE on its mRNA. The mutant luciferase reporter contains the TNFα ARE on its mRNA. B. After 24 hours of transfection with the luciferase reporters, RNA was isolated from HeLa cells, and converted to cDNA via reverse transcription PCR. The graph shows the QPCR of the cDNA. (Courtesy Dr. Shuping Gu.)

Current Study

We propose that all mutations reported in HSPB1, HSPB3, and HSPB8 affect the same cellular pathway because they all lead to the same clinical phenotype. It may be that these mutations act by a common mechanism to cause dHMN, even if they have different immediate effects in the cells. To determine how mutations in these different sHSPs lead to dHMN, we studied whether RNA processing is the relevant defect in dHMN. Since it

is clear that wild-type HSPB1 plays a role in ARE-mediated mRNA decay [12-14] and we have preliminary evidence that mutant HSPB1(R136W) alters ARE-mediated mRNA decay, we also looked at the function of wild-type and mutant HSPB3 in ARE-mediated mRNA decay. We hypothesized that the mutations in HSPB1 and HSPB3 affect ARE-mediated mRNA decay leading to a decrease in mRNA degradation, an increase in mRNA translation and protein expression, and ultimately the development of dHMN. Because mutations in genes associated with MNDs such as ALS, SMA, and lethal congenital contracture syndrome (LCCS) are involved in RNA processing, we studied RNA processing in a model of ALS in addition to models of dHMN [3]. Determining the effect of sHSP mutations on mRNA decay and the effect of an ALS model on mRNA decay will further help us to determine the mechanism of MNDs.

Hypothesis

We hypothesized that the HSPB1(R136W) and HSPB3(R7S) mutations will alter the activity and function of HSPB1 and HSPB3, respectively. Specifically, we hypothesized that HSPB1(R136W) and HSPB3(R7S) will affect the function of HSPB1 (and possibly HSPB3) in ARE-mediated mRNA decay, ultimately leading to dHMN. In addition, we hypothesized that ARE-mediated mRNA decay is altered *in vivo.*

Specific Aims

Mutations in HSPB1 and HSPB3 result in dHMN [7, 9]. It is known that HSPB1 is required for ARE-mediated mRNA decay [14]. To determine the relevant functional consequences of these mutations, I proposed the following specific aims:

Aim 1. To determine the effect of HSPB1 mutations on ARE-mediated mRNA decay. I measured the rate of mRNA decay of ARE-containing mRNAs and compared the rates of mRNA decay in the presence of wild-type or mutant HSPB1.

Aim 2. To determine whether ARE-mediated mRNA decay is altered *in vivo*. I helped develop a murine model of dHMN which will be used in future *in vivo* studies of ARE-mediated mRNA decay.

Aim 3. To determine whether ARE-mediated mRNA decay is altered by the expression of HSPB3. I will measure the decay rate of an ARE-containing mRNA in the presence of wild-type or mutant HSPB3.

Aim 1. To determine the effect of HSPB1 mutations on ARE-mediated mRNA decay.

Mutations in HSPB1 are known to cause dHMN [7]. It is known that HSPB1 is involved in ARE-mediated mRNA decay [14]. We have preliminary results showing that the disease-causing mutation, HSPB1(R136W), leads to overexpression of proteins, indicating that HSPB1(R136W) may inhibit ARE-mediated mRNA decay (unpublished data) (Figure 3). However, these preliminary experiments measured mRNA decay indirectly. Therefore, here, to determine the effect of HSPB1(R136W) on mRNA decay, we measured mRNA decay directly. We used QPCR to measure the levels of TNFα mRNA, an ARE-containing mRNA, from mouse macrophages that endogenously express TNFα. We measured the levels of TNFα mRNA at different time points, and thus were able to directly measure the rate of ARE-mediated mRNA decay. We hypothesized that HSPB1(R136W) inhibits ARE-mediated mRNA decay, and that this inhibition contributes to the mechanism of dHMN. Determining the effect of mutant HSPB1 on ARE-mediated mRNA decay will help us determine whether altered ARE-mediated mRNA decay is part of the mechanism of HSPB1 mutations leading to dHMN.

Aim 2: To *determine whether ARE-mediated mRNA decay is altered in vivo.*

Performing the ARE-mRNA decay assay on mouse macrophages helps to determine the role of sHSP mutations on mRNA decay *in vitro*. However, we also aim to determine the effect of sHSP mutations on mRNA decay *in vivo*. To determine the function of the HSPB1(R136W) mutation on mRNA decay *in vivo*, I have spent much of my early work in the lab developing a novel mouse model of the HSPB1(R136W)

mutation. These mice exhibited no difference in longevity, motor activity, or behavior compared to wild-type HSPB1 transgenic and non-transgenic control mice. However, they did show electrophysiological and pathological evidence of a subclinical axonal neuropathy. In the future, we will use these transgenic mice to determine the effect of the HSPB1(R136W) mutation on ARE-mediated mRNA decay *in vivo* by directly measuring the rate of mRNA decay from tissue samples from these animals. Determining whether HSPB1(R136W) leads to altered ARE-mediated mRNA decay *in vivo* will give us further evidence as to whether or not ARE-mediated mRNA decay contributes to the mechanism of dHMN caused by mutations in HSPB1.

Aim 3: To determine whether ARE-mediated mRNA decay is altered by the expression of HSPB3

Since HSPB3 is homologous to HSPB1 and HSPB8, we believe that the HSPB3(R7S) mutation leads to the same functional consequences, and thus acts by the same mechanism as the mutations in HSPB1 and HSPB8 to cause dHMN. However, little is known about the function of HSPB3. Therefore, we have begun to characterize wild-type and mutant HSPB3. We have determined the subcellular localization of wild-type HSPB3 and mutant HSPB3(R7S). In the future, we plan to determine whether HSPB3 functions in ARE-mediated mRNA decay and how HSPB3(R7S) alters that function. We will perform the same assays as in Aim 1, but with HSPB3 and HSPB3(R7S) instead of wild-type and mutant HSPB1. We hypothesize that wild-type HSPB3 will lead to ARE-mediated mRNA decay compared to untransfected cells, and

HSPB3(R7S) will lead to a deficiency in ARE-mediated mRNA decay compared to cells overexpressing wild-type HSPB3. Determining the effect of mutant and wild-type HSPB3 will help us to determine whether ARE-mediated mRNA decay is likely part of the common pathway of sHSP mutations causing dHMN.

Chapter 2

Materials and Methods

Harvesting Macrophages

Bone marrow derived macrophages were harvested from a mouse according to the Popovich lab protocol (Courtesy Dr. Phillip Popovich). A mouse was anesthetized with approximately 0.7 ml ketamine HCL/xylazine HCl solution (Sigma) and then euthanized by cervical dislocation. Alternatively, some mice were euthanized by CO_2 and then cervical dislocation. Then, the femur and tibia were flushed with DMEM/F12 + Glutamax media (Gibco) or PBS (Gibco). The media/cell solution was centrifuged at 1200 rpm for 5 minutes. The red blood cells were then lysed and removed from the bone marrow cells. The bone marrow cells were plated onto 10 cm dishes (Corning) in Advanced DMEM/F12 reduced serum (Gibco) with recombinant mouse granulocyte macrophage colony stimulating factor (0.1µg/ml), 5% L-glutamine (Cellgro), 10% FBS (Gibco), and 1% penicillin/streptomycin (Cellgro) and cultured at 37°C for at least 7 days.

Macrophage Stimulation

Macrophages were seeded into 6 well plates and left overnight. Macrophages were stimulated with lipopolysaccharide (LPS) (1 µg/ml) for 2 hours. Then, transcription

was stopped with actinomycin D (5 µg/ml) (Sigma). Cells were collected before actinomycin D and at various time points after the addition of Actinomycin D.

RNA isolation and conversion to cDNA

The RNA was isolated from the macrophages with the RNAqueous-4 PCR kit (Ambion). RNA (13.2µl/PCR reaction) was then converted to cDNA with the High Capacity cDNA Reverse Transcription kit using the included RT random primers (Applied Biosystems). The RT PCR cycles were 25°C for 10 min, 37°C for 120 min, and 85°C for 5 min.

Measurement of RNA decay rate

The RT PCR product was purified using the QIAquick PCR purification kit (Qiagen). Quantitative PCR was then performed on the purified cDNA using SYBR green master mix (Applied Biosystems) to detect TNFα cDNA. Each reaction mixture contained 10 µl 2x SYBR green master mix (Applied Biosystems), 1 µl primer-F (mSP-TNFα-F: 5'-GATTATGGCTCAGGGTCCAA-3' or mSP-GAPDH-F: 5'-CCACCCAGAAGACTGTGGAT-3') (1µM), 1 µl primer-R (mSP-TNFα-R: 5'-CTCCCTTTGCAGAACTCAGG-3' or mSP-GAPDH-R: 5'-CACATTGGGGGTAGGAACAC-3') (1 µM), 6 µl H2O, and 2 µl cDNA. The QPCR cycles were stage 1 (50°C for 2 min) once, stage 2 (95°C for 10 min) once, stage 3 (95°C for 15 seconds then 60°C for 1 minute) 40 times, then stage 4 (dissociation stage) (95°C for 15 seconds, 60°C for 1 minute, 95° for 15 seconds, 60°C for 15 seconds) once.

GAPDH was measured as the internal control gene. The Ct values were then converted into relative levels of TNFα mRNA normalized to GAPDH at the different time points after the addition of actinomycin D.

Transfection paradigm for measuring rate of mRNA decay

293 T cells were cultured in DMEM (Gibco) with 10% FBS (Gibco), and 1% penicillin/streptomycin. To make the lenti-virus containing the human HSPB1 gene, the 293 T cells were transfected with MDL, REV, VSV-G (viral genes), and a pBOB vector (Addgene) containing either the wild-type HSPB1 or mutant HSPB1 gene for 6 hours. The supernatant containing the virus was collected over 3 days. The virus was pelleted and resuspended in PBS with 10% glycerol. The macrophages were then transfected with the virus containing the mutant or wild-type HSPB1 gene for 40 hours.

Western Blot

The macrophages were harvested after the transfection and centrifuged at 1200 rpm for 10 minutes at room temperature. The cell pellets were resuspended in RSB-100 + 0.1% NP40. The cells were lysed via sonication and centrifuged at 14000 rpm for 15 minutes at 4°C. The cytoplasmic extracts were then used for the immunoblot and loaded into each lane of the polyacrylamide gel. The proteins were separated via sodium dodecyl sulfate polyacrylamide gel electrophoresis and transferred to a nitrocellulose membrane. The membrane was blocked with 3% BSA + 0.1Tx-100 in PBS. All

antibodies were diluted in blocking solution. GAPDH was used as the loading control. The bands were visualized with a LI-COR Odyssey Infrared Imager.

Transgenic Mice

The open reading from M13-HSPB1 (GeneCopoeia, Rockville, MD) was cut out of the HSPB1 gene and ligated into a MoPrP.*Xho* vector via digestion with *Xho*I [16]. Restriction endonuclease digestion was used to map the HSPB1 insert in the vector. DNA sequencing of the insert was used to determine its orientation (primers: forward: 5'-TACCCGCATAGCCGCCTCTT-3', reverse: 5'-GATGGTGATCTCGTTGGACT-3'). To linearize the vector with the insert, *Not*I was used to digest the vector, which was then purified via agarose gel chromatography. The digested and linear DNA was injected into fertilized oocytes, according to the standard techniques used at the Transgenic Animal Facility at The Ohio State University, Columbus, OH. PCR was used to determine which mice contained the HSPB1 transgene (PrP-HSPB1 primers: Forward 5'-CACTGGCTGATGACAGACTC-3'; Reverse 5'- CCGGTGTGGACCCCACCCAA-3'). The HSPB1(R136W) transgene was developed by making a single nucleotide substitution (C406T) with a commercially available kit (Stratagene, La Jolla, CA). Mice were cared for according to the *Principles of Laboratory Animal Care* (National Institutes of Health publication number 86-23) and the Ohio State University animal care committee guidelines.

Immunohistochemistry

Mice were anesthetized and perfused first with PBS, then with 4% paraformaldehyde in PBS. The sciatic nerve and lumbar sections of the spinal cord were removed and fixed in 4% paraformaldehyde in PBS at 4°C overnight. Transverese-free-floating sections 40 µm thick were sectioned with the Vibrotim 3000. The sections were blocked in 10% donkey serum in 0.1% Triton X-100 in PBS at room temperature for 2 hours. Then, the sections were incubated in diluted primary antibody at 4°C overnight. The sections were then incubated in a 1:200 dilution of Alexa Fluor ® secondary antibodies (Invitrogen, Carlsbad, CA) at room temperature for 2 hours. Primary and secondary antibodies were diluted in 10% donkey serum in 0.1% Triton X-100 in PBS. 0.1M PBS was used to rinse the sections. The sections were coverslipped with Immumount (Thermo Scientific, Pittsburgh, PA). A Zeiss LSM510-META confocal laser-scanning microscope (Zeiss, Thornwood, NY) was used to take images.

Electrophysiology

Conduction studies of the caudal tail nerve and sciatic motor nerve were conducted as previously described [17]. Mice were anesthetized via interperitoneal injection of 100 mg/kg ketamine + 10 mg/kg xylazine (Sigma-Aldrich, St. Louis, Missouri). The distal back and hindlimbs of the mice were shaved. Hair-removal cream removed excess fur not removed via shaving. Water and alcohol were used to clean the exposed skin. Mice were restrained with tape on a piece of styrafoam with their hindlimbs extended at the knees and abducted at the hips. Disposable 27G needle

electrodes (Ambu USA, Glen Burnie, Maryland) were used to stimulate the mice and ring electrodes (Alpine Biomed, Skoylunde, Denmark) were used to record the electrical conduction. The mice were grounded through their tail via a disposable disc surface electrode, (Ambu USA, Glen Burnie, Maryland). A portable electrodiagnostic system (Synergy EMG machine version 9.1, Oxford Instruments, Abingdon, UK) was used to perform motor nerve conduction studies NCS. An LCD monitor (Toshiba Northa America, Houston, Texas) was used to show the waveforms. The high and low pass filters were set at 10 kHz and 0 Hz, respectively. The recording ring electrodes were coated with electrode gel (Spectra 360 by Parker laboratories, Fairfield, New Jersey) and placed at the base of the tail for tail motor NCS. The reference electrode was 10 mm distal to the ring electrode. The cathode used for stimulation was inserted 2-3 mm deep. This cathode was place 5 mm proximal to the recording electrodes and 3-5 mm lateral to the midline in order to generate distal responses. It was then moved 7 mm away from the distal stimulating point to generate proximal responses. The anode was placed subcutaneously in the skin overlying the sacrum. 0.1-ms single square-wave pulses stimulated the nerve. Gradually, supramaximal responses were generated, and maximal responses were obtained with stimulus currents of less than 10 mA. A tape measure was used to measure the distance between the proximal and distal sites of stimulation. Sensitivity of 20 mV/division and sweep speed of 2 ms/division were used to gather the data. For every studied nerve, the distal latency, distal and proximal compound motor action potential (CMAP) amplitudes, distal and proximal CMAP durations (measured from onset of initial negative deflection to initial return to baseline), and conduction

velocity were measured. To study the contralateral side, the electrodes used for stimulation were moved without altering the position of the recording electrodes. For the sciatic nerve (ScN) motor NCS, the active recording ring electrode was placed over the gastrocnemium muscle with the reference electrode over its tendon. The stimulating cathode was placed 5 mm proximal to the recording electrode in the midline of the posterior thigh and 6 mm proximally in the medial gluteal region to obtain distal and proximal responses, respectively. The anode was placed subcutaneously in the midline over the sacrum. The mice were stimulated, and electrophysiological data were acquired as described previously for the tail motor NCS.

Behavioral testing

The mice were weighed monthly for 1 year. Their hindlimb muscle strength was also tested monthly for 1 year by holding them by the tail and observing the spread of their hind limbs due to reflex. At 6 months old, the mice were placed in an open field Digiscan Activity Monitor (Accuscan, Columbus, OH) for 2 hours. The motion and activity of the mice was measured by the Accuscan software according to breaks in 16 light beams on the horizontal X and Y plane. To measure leg weakness and to determine how the transgenes affected the gait of the mice, the footprints of the mice were analyzed. The hind paws were painted with ink. Then, the mouse was placed in a wooden corridor (6 cm x 40 cm) where they walked from beginning to end on a sheet of paper as described [18, 19]. The toe spread (TS) (the distance between the 1^{st} and 5^{th} toes), the

inter-toe spread (IT) (the distance between the 2nd and 4th toes), and the paw length (PL) of the footprints were measured.

Transfection paradigm for subcellular localization of HSPB3 and HSPB3(R7S)

HeLa cells were grown in minimum essential media (Gibco) with 10% fetal bovine serum (Gibco), 1% penicillin-streptomycin solution (Fisher), and 1% non-essential amino acids (Gibco). HeLa cells were seeded onto cover slides and grown over night to 70% confluency. The cells were then transiently-transfected with a pmaxGFP vector (Lonza) containing the green fluorescent protein gene or with a PCDNA/4TO vector that contained the flag-tagged HSPB3 gene, the flag-tagged HSPB3(R7S) gene, or the flag-tagged HSPB1 gene. The cells were transfected with the FuGENE HD transfection reagent (Roche) for 17 hours.

Immunofluorescence for subcellular localization of HSPB3 and HSPB3(R7S)

After transfection, the cells were fixed with 1% formaldehyde for 30 minutes and blocked with 4%BSA+0.5%TritonX-100 in PBS. Mouse-anti-flag antibody (Sigma) was the primary antibody and anti-mouse-Alexa Fluor-488 antibody (Invitrogen) was the secondary antibody. All antibodies were diluted in 4%BSA+0.1%TritonX-100 in PBS. Images were taken with a confocal microscope (courtesy of Dr. Raphael-Fortney).

Calculations

Primer Efficiencies

Primer efficiencies were determined from the slope of the standard curve. Seven serial dilutions of cDNA harvested from stimulated macrophages before the addition of actinomycin D were used to make the standard curve. Quantitative PCR was performed on the serial dilutions of cDNA using the QPCR reaction mixtures and cycles as stated above. The Ct values were plotted versus the dilution factor on a logarithmic scale to determine the standard curve. A logarithmic regression line was fitted to the plotted Ct values. The slope was used to determine the primer efficiencies according to the equation: Efficiency = $10^{(-1/\text{slope})}$.

Determination of mRNA levels and mRNA half life

QPCR was performed on the cDNA isolated at different time points post-addition of actinomycin D as state above. QPCR was used to quantitate the levels of TNFα cDNA and GAPDH cDNA. GAPDH was used as the internal control. TNFα was used to determine the rate of ARE-mediated mRNA decay. Since TNFα is endogenously expressed in macrophages and has an ARE on its mRNA, measurement of TNFα mRNA is an ideal mRNA to detect when studying ARE-mediated mRNA decay. The Ct values were converted to fold changes of mRNA over time post-actinomycin D for either TNFα or GAPDH according to the equation: Fold Change = $\text{efficiency}^{(\text{Ct at time 0})-(\text{Ct at time t})}$ where time t is hours post-addition of actinomycin D, and time 0 is the time at which actinomycin D was added. The TNFα fold changes were normalized to GAPDH by

dividing the fold change of TNFα mRNA by the fold change of GAPDH mRNA for the same time point. The comparison of this ratio at different time points represented the relative levels of TNFα mRNA at those time points. The scatter plot of the relative levels of TNFα mRNA was fitted with an exponential regression equation of the form: $y=y_0e^{-kt}$. The half lives of TNFα mRNA under different conditions were calculated according to the equation: $t_{1/2}=\ln 2/k$.

Results

Aim 1.To determine the effect of HSPB1 mutations on ARE-mediated mRNA decay

Harvesting Macrophages

After bone marrow cells were harvested from mice and cultured for 10 days, we determined that these cultured cells were macrophages by detection of cd11b (Figure 4). Cd11b is the alpha chain of the Mac-1 leukocyte integrin heterodimer [20]. Cd11b is an adhesion molecule that is expressed at high levels in macrophages, monocytes, and neutrophils, but is either not detectable or has very low expression in myeloid precursor cells [20]. Therefore, we used cd11b as a macrophage marker.

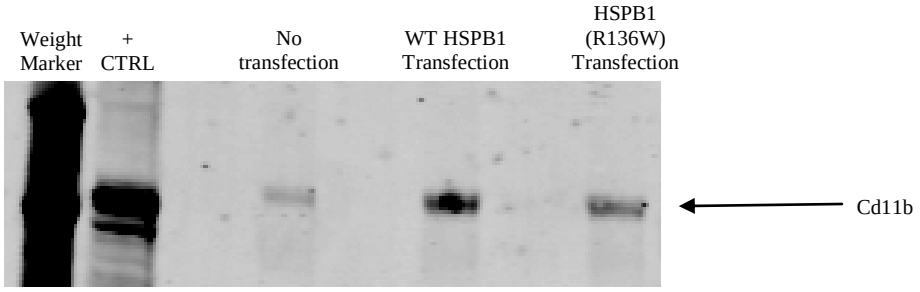

Figure 4. Cultured mouse bone marrow cells are macrophages.

Bone marrow cells were harvested from mice and cultured for 10 days. The bone marrow cells were then harvested and a western blot was performed on these cells to confirm that they were macrophages via detection of cd11b. The primary antibody was rabbit-anti cd11b (abcam 1:1000 dilution). The secondary antibody was goat-anti rabbit (Odyssey; 1:10000 dilution).

Development of the RNA decay assay

To develop the RNA decay QPCR assay, a standard curve was made with serial dilutions of cDNA. The primer efficiencies were calculated from the standard curve to be 4.73888 for the TNFα primers and 4.753878 for the GAPDH primers (Figure 2 and Table 1).

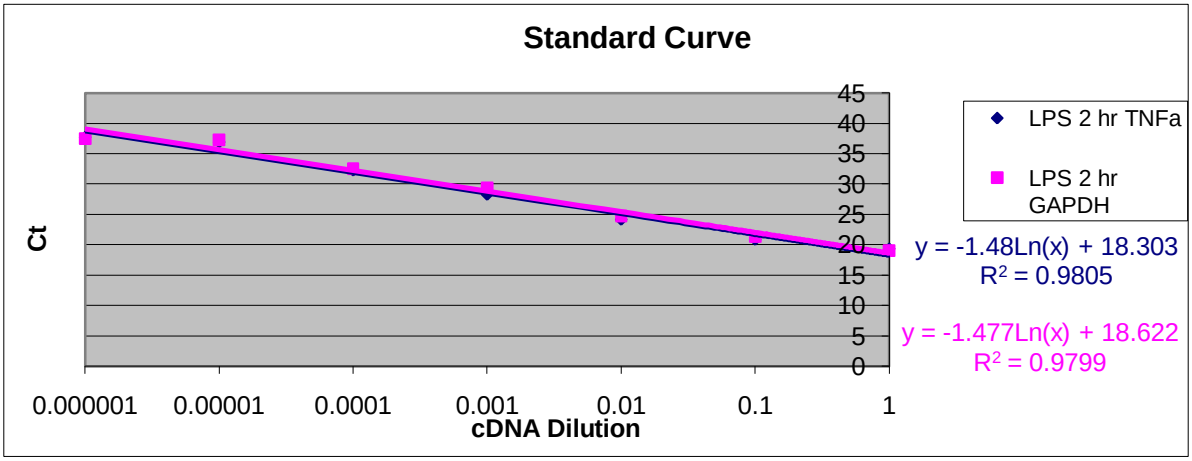

Figure 5. Standard curve for QPCR primers.

$1.83x10^5$ macrophages/well were plated into 6 well plates and left overnight. The macrophages were stimulated with LPS (1 µg/ml) for 2 hours and then collected. RNA was isolated and converted to cDNA. Quantitative PCR was then performed on seven serial dilutions of cDNA to make a standard curve. Standard curves were made for the TNFα primers (the experimental gene) and GAPDH primers (the internal control gene).

Primers	Slope	Primer Efficiency
TNFα	-1.48	4.73888
GAPDH	-1.477	4.753878

Table 1. TNFα and GAPDH primer efficiencies.

The slope of the regression line of the standard curve was used to calculate the efficiency of each primer pair according to the equation: efficiency = $10^{-1/slope}$.

Since, TNFα is endogenously expressed in macrophages and has an ARE on its mRNA, measurement of TNFα mRNA is an ideal mRNA to detect when studying ARE-mediated mRNA decay. To determine the rate of TNFα mRNA decay, and thus the rate of ARE-mediated mRNA decay, macrophages were stimulated for 2 hours with LPS (1µg/ml), actinomycin D (5µg/ml) (Sigma) was added to stop transcription, the macrophages were harvested at the indicated time points, and the rate of decay of TNFα mRNA was determined. After transcription was stopped, the TNFα mRNA decayed over time as shown by the gradual decline in relative levels of TNFα mRNA for the actinomycin D data in Figure 6. The half life of TNFα mRNA was calculated to be 16.94 minutes when actinomycin D was added. The half life of TNFα mRNA was calculated to be -84.9 minutes when actinomycin D was not added. We were able to confirm that a function of actinomycin D is to stop transcription. Upon the addition of actinomycin D, the relative level of TNFα mRNA decreased because no new TNFα mRNA was being transcribed and the TNFα mRNA that was present decayed normally. However, when actinomycin D was not added, the levels of TNFα mRNA did not decrease because the natural decay of TNFα mRNA was being offset by the transcription of new TNFα mRNA.

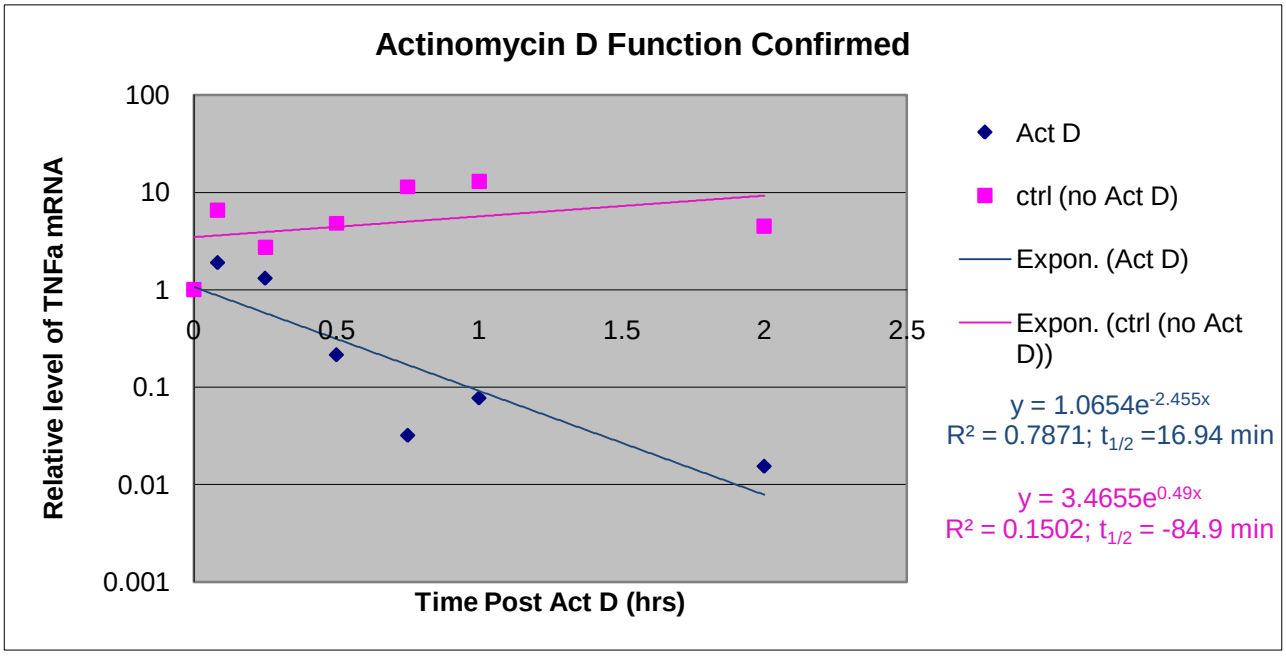

Figure 6. Actinomycin D confirmed to inhibit transcription, allowing the rate of mRNA decay to be measured.

$1.83x10^5$ macrophages/well were plated into 6 well plates and left overnight. The cells were stimulated with LPS (1 µg/ml) for 2 hours. Then transcription was stopped with Actinomycin D (5 µg/ml). Macrophages were collected before the addition of actinomycin D (time 0), and 5 minutes, 15 minutes, 30 minutes, 45 minutes, 1 hour, and 2 hours after the addition of actinomycin D. Control macrophages (with no Actinomycin D) were stimulated with LPS and collected simultaneously. RNA was isolated and converted to cDNA which was quantitated via QPCR. Fold changes of TNFα cDNA over time were normalized to fold changes of GAPDH over time. This ratio represented the relative levels of TNFα mRNA at the indicated time points. The half life of TNFα mRNA with or without the addition of actinomycin D was calculated from the exponential regression equation.

ARE-mediated mRNA decay in macrophages transfected with mutant or wild-type HSPB1

Macrophages were transfected with either the wild-type HSPB1 gene or the mutant HSPB1(R136W) gene (Figure 7). To date, we have had difficulties obtaining a robust transfection efficiency and have been unable to address the effect of mutant HSPB1 on ARE-dependent mRNA decay in macrophages.

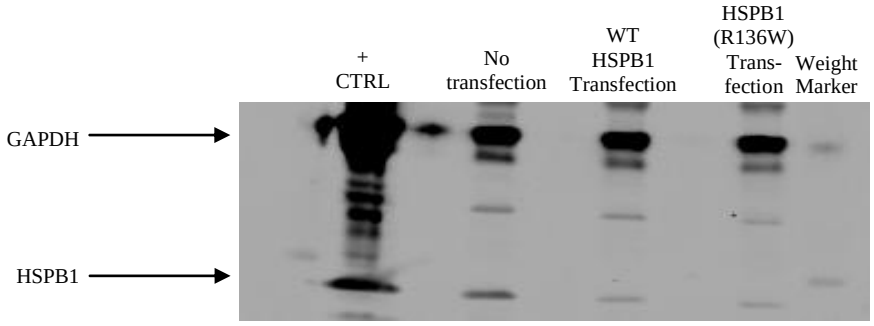

Figure 7. Unsuccessful lenti-viral transfection of macrophages with HSPB1 and HSPB1(R136W).

$1.7x10^5$ mouse macrophages/well were transfected with a lenti-viral vector containing a wild-type HSPB1 gene or a mutant HSPB1(R136W) gene. 40 hours post-transfection, the cells were harvested for a western blot to determine if the exogenous HSPB1 and HSPB1(R136W) were expressed. GAPDH was detected as a loading control. The primary antibodies were mouse-anti Hsp27 (abcam; 1:500 dilution) for HSPB1 and mouse-anti GAPDH (Ambion; 1:4000 dilution.) The secondary antibody was goat-anti mouse (Odyssey; 1:10000 dilution).

40 hours post-transfection, the mRNA decay assay was performed on these cells (Figure 8). The half-life of TNFα mRNA was calculated to be 43.5 minutes for untransfected macrophages, 7.81 minutes for macrophages transfected with the wild-type HSPB1 gene, and 8.87 min for macrophages transfected with the HSPB1(R136W) gene.

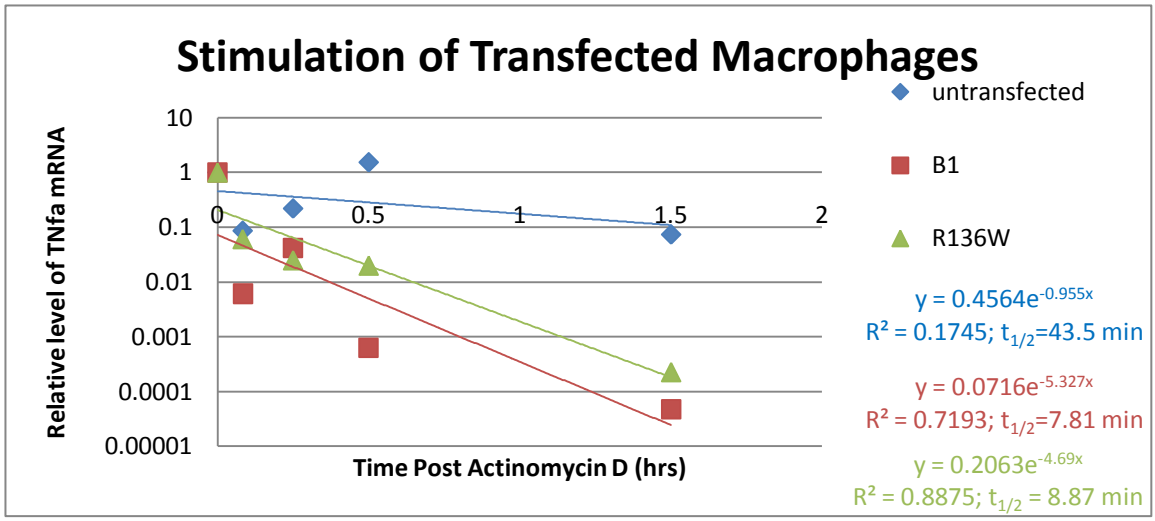

Figure 8. TNFα mRNA decay of cells transfected with HSPB1 or HSPB1(R136W) genes.

$1.7x10^5$ macrophages/well were plated into 6 well plates and left overnight. The macrophages were transfected with a lenti-viral vector containing the HSPB1 gene or the HSPB1(R136W) gene. Untransfected cells were used as a control. 40 hours post-transfection, the cells were stimulated with LPS (1 µg/ml) for 2 hours. Then transcription was stopped with Actinomycin D (5 µg/ml). Macrophages were collected before the addition of actinomycin D (time 0), and 5 minutes, 15 minutes, 30 minutes, and 1.5 hours after the addition of actinomycin D. RNA was isolated and converted to cDNA which was quantitated via QPCR. Fold changes of TNFα cDNA over time were normalized to fold changes of GAPDH over time. This ratio represented the relative levels of TNFα mRNA at the indicated time points. The half life of TNFα mRNA was calculated from the exponential regression equations.

Aim 2: To determine whether ARE-mediated mRNA decay is altered in vivo

Expression and localization of HSPB1 and HSPB1(R136W) transgenes

To complete this Aim, our laboratory created novel transgenic mouse lines expressing wild-type HSPB1 or mutant HSPB1. HSPB1 and HSPB1(R136W) were expressed in both the brain and the spinal cord, including the ventral horn of the spinal cord in ChAT-positive neurons, with no apparent difference in subcellular localization between mutant and wild-type HSPB1 (Figure 9). Neither wild-type HSPB1 nor

HSPB1(R136W) was expressed in glial cells of the spinal cord, indicating that the PrP promoter is neuronal-specific. Interestingly, expression of wild-type HSPB1 was lower than the expression of HSPB1(R136W) in both brain and spinal cord.

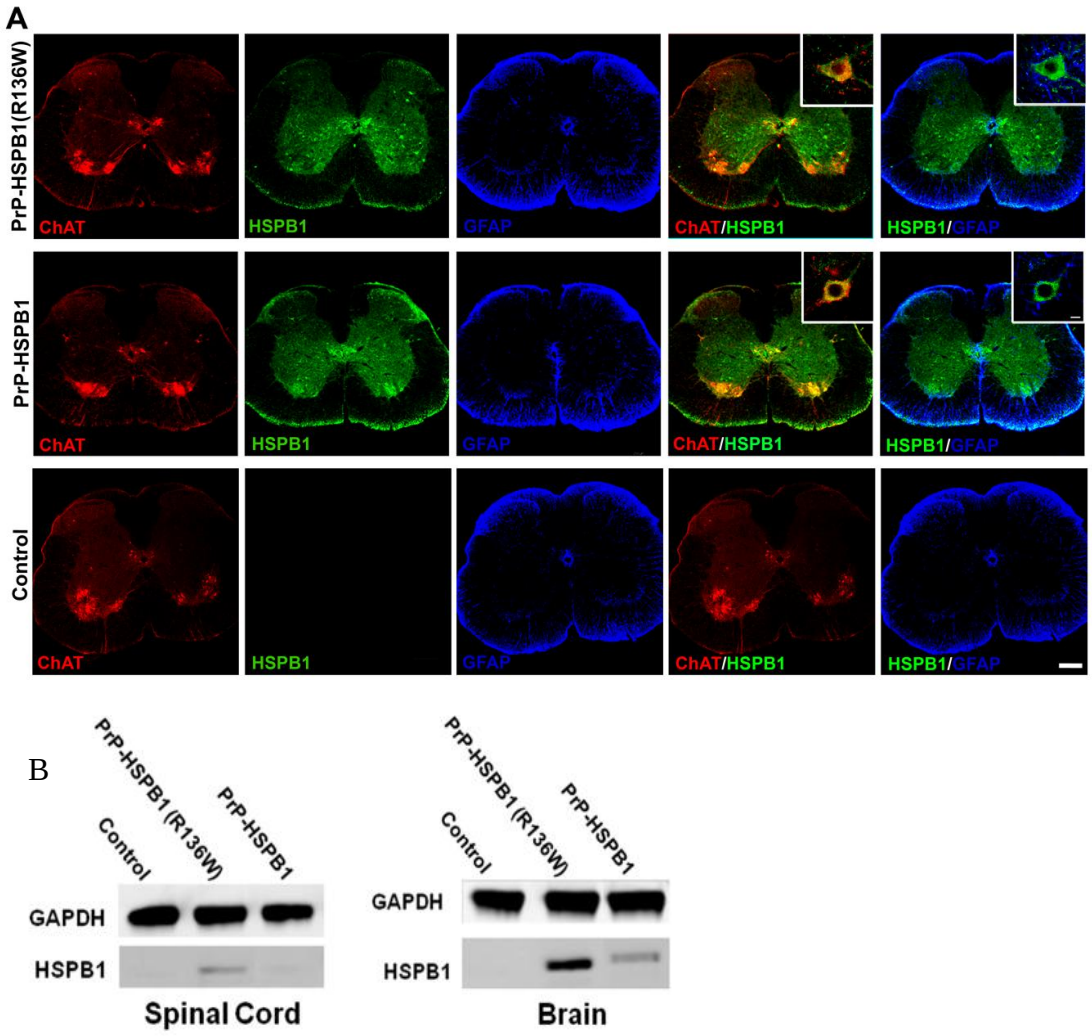

Figure 9. Expression of HSPB1(R136W) and HSPB1 transgenes.

A) Both the HSPB1 and HSPB1(R136W) transgenes (green) are expressed in the ventral horn of the spinal cord in ChAT positive neurons (red). Neither transgene is expressed in glial cells (blue). Nontransgenic FVB mice do not express HSPB1 in neurons or glial cells (Courtesy Dr. Amit Srivastava.) B) Brain and spinal cord samples were harvested from HSPB1 and HSPB1(R136W) transgenic mice. Samples were also harvested from non-transgenic mice as a control. Expression of HSPB1 or HSPB1(R136W) was detected via western blot. The primary antibodies were rabbit-anti Hsp27 (abcam; 1:1000 dilution) for HSPB1 and mouse-anti-GAPDH (ambion; 1:4000 dilution). The secondary antibodies were goat-anti mouse (Odyssey; 1:10000 dilution) and goat-anti rabbit (Odyssey; 1:10000 dilution) (Courtesy Samantha Renusch).

Because dHMN caused by sHSP mutations is an axonal neuropathy in humans, we wanted to show if in our model, the expressed wild-type HSPB1 and HSPB1(R136W) proteins were transported from the motor neuron cell body to the axons of the peripheral nervous system. In both transgenic animals, wild-type and mutant HSPB1 showed co-localization with neurofilaments showing that these proteins are transported to axons in the peripheral nervous system (Figure 10).

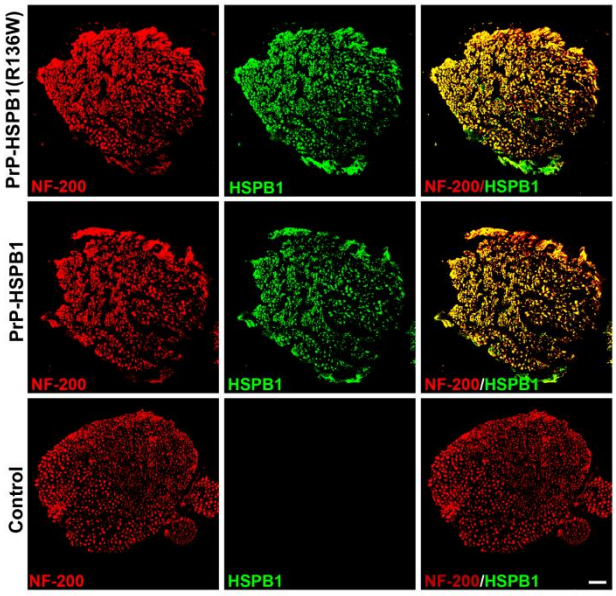

Figure 10. Co-localization of wild-type HSPB1 and HSPB1(R136W) with neurofilaments.

Wild-type and mutant HSPB1 (green) are expressed in neurofilament-containing neurons (red) in the sciatic nerves from transgenic mice. Scale bar, 50μm. (Courtesy Dr. Amit Srivastava.)

HSPB1(R136W) leads to a decrease in axonal conduction

To determine if HSPB1(R136W) led to an axonal or a demyelinating neuropathy, electrophysiolocial studies were conducted on the transgenic mice at 6 months and 1 year of age (Figure 11.) At 6 months, there were no statistically significant differences between sciatic motor amplitudes of the non-transgenic control, transgenic HSPB1, or transgenic HSPB1(R136W) mice. At 1 year old, the transgenic HSPB1(R136W) showed a statistically significant decrease in sciatic motor amplitude ($p<0.05$) compared to transgenic HSPB1 and non-transgenic mice. However, there was no statistically significant difference in the conduction velocity of the HSPB1 transgenic, HSPB1(R136W) transgenic, or non-transgenic mice. This indicates that the transgenic HSPB1(R136W) mice developed an axonal neuropathy by 1 year of age.

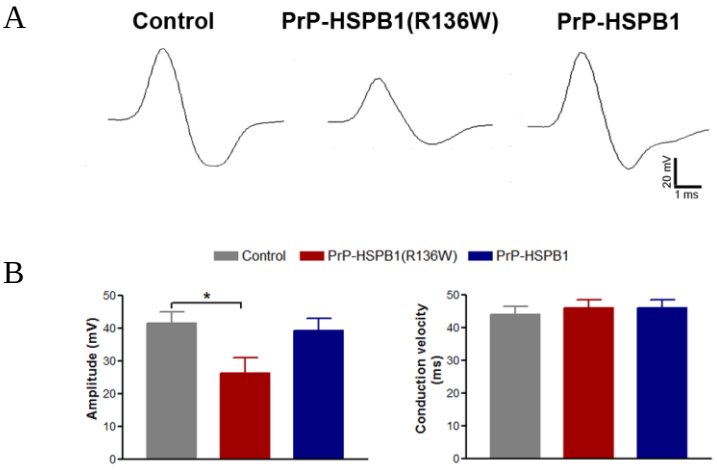

Figure 11. Electrophysiology of transgenic mice.

A) Waveforms of electrophysiological stimulation of non-transgenic control, transgenic PrP-HSPB1(R136W), and transgenic PrP-HSPB1 mice at 1 year of age. B) Quantitation of amplitude and conduction velocity of electrophysiological waveforms in A (Courtesy Dr. David Arnold). N=5 for each group of mice.

Behavioral analysis

There was no significant difference in the mortality rate of transgenic HSPB1(6.53% mortality), transgenic HSPB1(R136W) (6.11% mortality), and nontransgenic (9.31% mortality) mice. An open field Plexiglas chamber with light sensors was used to measure the motion and activity of the mice. The behavior of the transgenic HSPB1, transgenic HSPB1(R136W), and non-transgenic mice were not significantly different at 6 months of age (Table 2).

	Prp-HSPB1	**Prp-HSPB1(R136W)**	**FVB/NJ**	**p-value**
Total distance (cm.)	9330 ± 6197	20718± 47224	26540 ± 43136	0.81
Rest time (sec.)	5376 ± 1403	5378± 1173	5255 ± 1354	0.93
Movement time (sec.)	1823 ± 1402	1820 ± 1173	1944 ± 1354	0.93
Sterotypy count	565 ± 465	560 ± 377	547 ± 416	0.99
Vertical activity time (sec.)	1031 ± 863	573 ± 370	559 ± 424	0.3
Vertical activity count	2110 ± 1224	1481 ± 912	1538 ± 1203	0.72
Wheel rotations	1130 ± 985	408 ± 432	667 ± 818	0.17

Table 2. Difference in behavior among transgenic HSPB1, transgenic HSPB1(R136W), and non-transgenic mice.

At 6 months of age, transgenic HSPB1, transgenic HSPB1(R136W), and nontransgenic mice were placed in an open field activity box for 2 hours. Different parameters describing the behavior and activity of the mice were measured. Data expressed as mean ± S.D. One-way ANOVA. $p<0.05$ is considered significant. N=24 for non-transgenic control mice; N=27 for PrP-HSPB1(R136W) mice; N=2 for PrP-HSPB1 mice.

The footprints of 1 year old mice were measured and analyzed. There was no statistically significant difference between mutant PrP-HSPB1(R136W), wild-type PrP-HSPB1, or non-transgenic mice toe spread, inter-toe spread, or paw length (Figure 12).

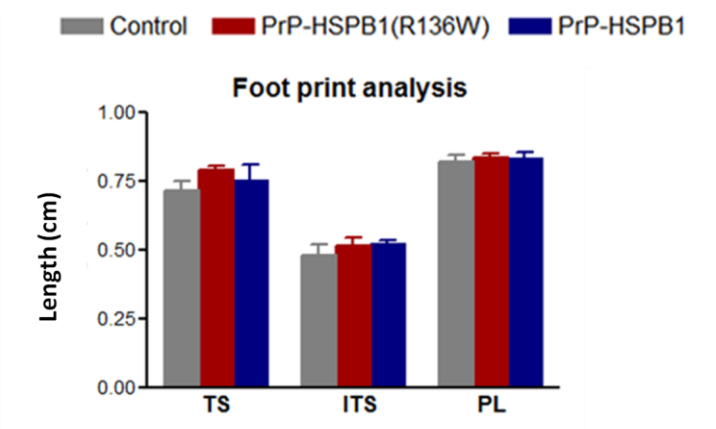

Figure 12. Foot print analysis of 1 year old nontransgenic, transgenic HSPB1, and transgenic HSPB1(R136W) mice.

Toe spread (TS), inter-toe spread (ITS), and paw length (PL) of 1 year old nontransgenic, transgenic HSPB1, and transgenic HSPB1(R136W) mice were measured. There was no statistically significant difference between nontransgenic, transgenic HSPB1, and transgenic HSPB1(R136W) foot prints. N=5 for each group of mice.

Aim 3: To determine whether ARE-mediated mRNA decay is altered by the expression of HSPB3

Little is known about the function of wild-type HSPB3. To begin to characterize both wild-type and mutant HSPB3, we determined the subcellular localization of HSPB3 and HSPB3(R7S). We transiently transfected HeLa cells with either PCDNA4/TO-FB3, PCDNA4/TO-FR7S, PCDNA4/TO-FB1, or pmaxGFP and then performed immunofluroescence on the cells (Figure 13). HSPB1 is known to be a cytoplasmic

protein, and since HSPB1 is homologous to HSPB3, we wanted to compare the subcellular localization of HSPB3 to HSPB1 [21]. We used GFP as a transfection control to show that our transfection procedure was working. GFP was successfully expressed throughout the cells (Figure 13A). We preliminarily confirmed that HSPB1 is a cytoplasmic protein (Figure 13B). However, our preliminary results showed that HSPB3 and HSPB3(R7S) are localized in the nucleus, but not in the nucleolus (Figure 13C, 13D). There was no significant difference between the subcellular localization of HSPB3 and HSPB3(R7S) (Figure 13C, 13D).

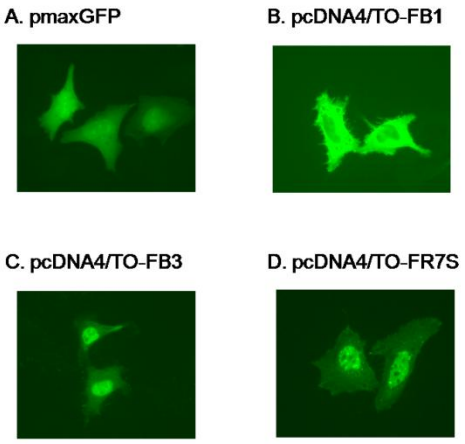

Figure 13. Subcellular localization of mutant and wild-type HSPB3.

Immunofluorescence of HeLa Cells transiently transfected with pmaxGFP or with the pcDNA4/TO vector containing flag-tagged genes for HSPB1, HSPB3, or HSPB3(R7S). The green shows GFP and the anti-flag antibody which recognized HSPB1, HSPB3, and HSPB3(R7S). A) HeLa cells transfected with pmaxGFP containing the GFP gene. B) HeLa cells transfected with pcDNA4/TO-FB1 containing the flag-tagged HSPB1 gene. C) HeLa cells transfected with pcDNA4/TO-FB3 containing the flag-tagged HSPB3 gene. D) HeLa cells transfected with pcDNA4/TO-FR7S containing the flag-tagged HSPB3(R7S) gene.

HSPB3 is very difficult to transfect. As a result, the other preliminary experiments of HSPB3 expression were unsuccessful, and we did not have time to perform the ARE-

mediated mRNA decay assay with macrophages expressing the HSPB3 or HSPB3(R7S) genes.

Chapter 4

Discussion

Aim 1.To determine the effect of HSPB1 mutations on ARE-mediated mRNA decay

We successfully developed an assay to measure the rate of mRNA decay (Figure 6). When actinomycin D was added to the macrophages, the TNFα mRNA decayed over time because transcription was inhibited. Without the addition of actinomycin D, the levels of TNFα mRNA did not decrease, as shown by a negative half-life, because TNFα mRNA was being continuously transcribed.

The results of the mRNA decay assay on the macrophages transfected with the HSPB1 gene or the HSPB1(R136W) gene were inconclusive. Expression of HSPB1 and HSPB1(R136W) was not detected in the western blot of the transfected macrophages, indicating that the transfection was unsuccessful (Figure 7). Also, HSPB1 and HSPB1(R136W) cDNA from transfected macrophages was not detected by QPCR (data not shown). However, the half-life of TNFα mRNA of the untransfected macrophages was over 5 times higher than that of the macrophages transfected with the HSPB1 or HSPB1(R136W) genes. Based on the failure of the western blot and QPCR to detect HSPB1 and HSPB1(R136W) protein and cDNA, respectively, it would seem that the transfection was unsuccessful. The transfection efficiency may have been too low to detect via western blot and QPCR. Therefore, when the transfection is repeated, a more sensitive method of protein expression detection, such as immunofluorescence staining,

should be used to detect HSPB1 and HSPB1(R136W) expression to determine the transfection efficiency.

If the case was that the transfection efficiency was too low to be detected via western blot and QPCR, but low levels of HSPB1 and HSPB1(R136W) were expressed, the results indicate that HSPB1(R136W) did not have an inhibitory effect on ARE-mediated mRNA decay because there was little difference between the TNFα mRNA half lives in macrophages transfected with wild-type HSPB1 and macrophages transfected with HSPB1(R136W). However, the half-life of TNFα mRNA was slightly higher in macrophages transfected with the HSPB1(R136W) gene than in macrophages transfected with the wild-type HSPB1 gene. This could indicate that HSPB1(R136W) does have an inhibitory effect on ARE-mediated mRNA decay, but the expression of HSPB1 and HSPB1(R136W) was too low to show the difference because of the poor transfection efficiency.

Another possibility to explain this contradiction is that the lenti-viral transfection reagents may have had an unanticipated effect on the mRNA decay machinery despite the lack of HSPB1 and HSPB1(R136W) expression. This would explain why there was a huge difference between the half-lives of TNFα mRNA of the transfected and untransfected macrophages, but little difference in half-lives between the macrophages transfected with the wild-type HSPB1 gene and those transfected with the HSPB1(R136W) gene. When this experiment is repeated the untransfected control macrophages should be infected with an empty lenti-viral vector to control for this unanticipated effect.

Also, the R^2 values for the exponential regression equations were all significantly less than 0.9. Therefore, the calculated half-lives may not be accurate. This experiment must be repeated multiple times until the data is reproducible and the R^2 values are closer to 1 before conclusions can be drawn about the affect of HSPB1(R136W) on ARE-mediated mRNA decay *in vitro*.

Role of ARE-mediated mRNA decay in other MNDs

All MNDs are related and are characterized by muscle weakness and motor neuron death. Because MNDs have related clinical phenotypes, we hypothesize that a common pathway is altered in all MNDs. Specifically, because ARE-mediated mRNA decay is implicated in dHMN, and other alterations of RNA processing are implicated in ALS, SMA, and lethal congenital contracture syndrome (LCCS) [3], we hypothesized that mRNA processing is altered in all MNDs. To determine if ARE-mediated mRNA decay, a specific type of mRNA processing, is affected in MNDs other than dHMN, we performed the ARE-mediated mRNA decay assay as described in Aim 1 on macrophages from a well established mouse model of ALS, in which there is a G93A mutation in superoxide dismutase 1 (SOD1) (courtesy of Dr. Glenn Lin) [22]. The SOD1 G93A mouse model is the most commonly used mouse model of ALS [23] (Figure 12). The wild-type mice had a TNFα mRNA half life of 13.4 minutes. The mutant G93A mice had a TNFα mRNA half life of 13.81 minutes. This indicates that ARE-mediated mRNA decay is not altered in this model of ALS; however, these results are only from one experiment, and are therefore preliminary.

In addition, the R^2 values for the exponential regression equations were below 0.6, possibly due to the presence of outliers. Therefore, this experiment must be repeated multiple times and further analyses must be done before conclusions can be made about the role, or lack thereof, of ARE-mediated mRNA decay in this model of ALS.

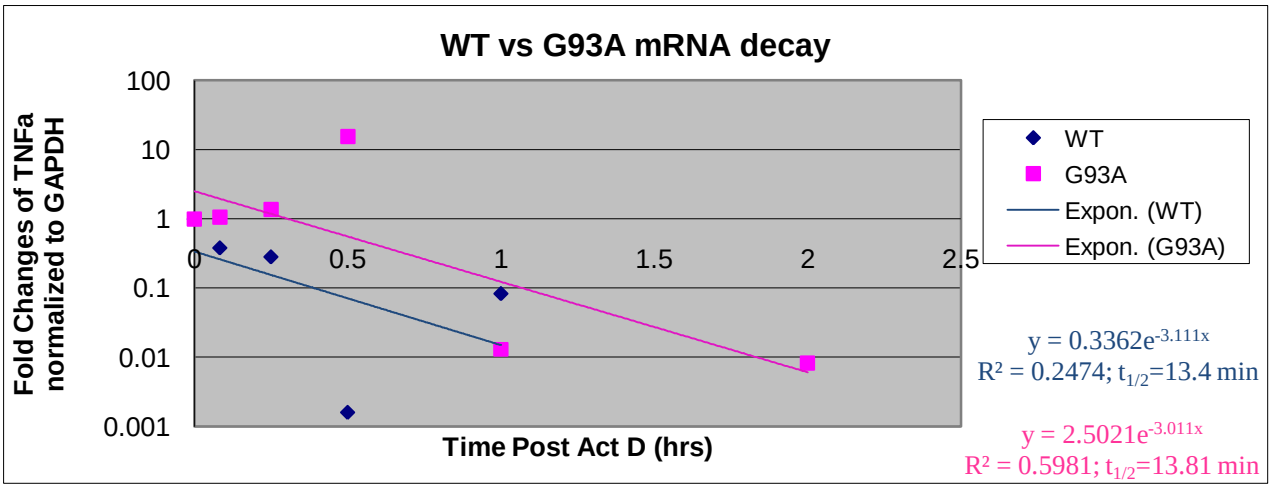

Figure 14. ARE-mediated mRNA decay is not inhibited in mouse model of ALS.

Macrophages were harvested from 2 wild-type mice and 2 mice containing the G93A mutation in SOD1 from a mouse model of ALS. $2.5x10^5$ macrophages/well were plated into 6 well plates and left overnight. The cells were stimulated with LPS (1 µg/ml) for 2 hours. Then transcription was stopped with Actinomycin D (5 µg/ml). Macrophages were collected before the addition of actinomycin D (time 0), and 5 minutes, 15 minutes, 30 minutes, 1 hour, and 2 hours after the addition of actinomycin D. RNA was isolated and converted to cDNA which was quantitated via QPCR. Fold changes of TNFα cDNA over time were normalized to fold changes of GAPDH over time. This ratio represented the relative levels of TNFα mRNA at the indicated time points. The half life of TNFα mRNA was calculated from the exponential regression equation

Aim 2: To determine whether ARE-mediated mRNA decay is altered in vivo

Both wild-type HSPB1 and HSPB1(R136W) were expressed in the brain, and spinal cord, including the ventral horn of the spinal cord. There was no significant

difference in subcellular localization between the wild-type and mutant HSPB1 protein. Both proteins were expressed in neurons of the spinal cord, but neither protein was expressed in glial cells of the spinal cord indicating that the PrP promoter limited transgene expression to neurons.

Both HSPB1 and HSPB1(R136W) showed co-localization with neurofilaments indicating that these proteins were being transported from the motor neuron cell bodies to the axons. This localization combined with the statistically significant decrease in sciatic motor amplitude of PrP-HSPB1(R136W) 1 year old mice compared to PrP-HSPB1 or non-transgenic control 1 year old mice indicates that the PrP-HSPB1(R136W) mice develop an axonal neuropathy. In addition, there was no statistically significant difference between conduction velocity of these mutant mice compared to wild-type and non-transgenic control mice. A difference in conduction velocity would have suggested a demylinating neuropathy unlike that seen in dHMN patients with sHSP mutations. However, this was not the case, further supporting the conclusion that these PrP-HSPB1(R136W) mice developed an axonal neuropathy.

Because there was no significant difference in the localization of HSPB1 expression between the two transgenic lines, and because there was little difference in behavior or gait between the mutant transgenic mice, the wild-type transgenic mice, and the non-transgenic mice, the axonal neuropathy developed was mild and subclinical, unlike that seen in patients. One reason that these mice did not develop a severe, clinical neuropathy may be that we used a prion-protein promoter to limit expression of the transgene to neurons. In patients, the sHSP mutations are expressed ubiquitously. In

patients, the HSPB1(R136W) expressed in non-neuronal cells may affect motor neurons in a non-cell autonomous manner. Therefore, HSPB1(R136W) may not have been expressed at high enough levels in non-neuronal cells for the development of a severe clinical neuropathy. This type of non-cell autonomous effect of non-neuronal cells on motor neurons is seen in the SOD1 model of ALS [24-26]. Another possibility as to why these PrP transgenic mice did not develop a clinical neuropathy may be that the endogenous mouse HSPB1 homolog, Hsp 25, was compensating for the harmful effects of the mutant HSPB1(R136W).

In order to determine whether ARE-mediated mRNA decay is affected *in vivo* in a model for dHMN, ARE-mediated mRNA decay must be measured directly from our mouse model of dHMN. Ideally, a transgenic HSPB1 mouse that exhibits a more severe phenotype would permit more confidence that any alterations in mRNA decay that may be found are related to the neuropathy.

Aim 3: To determine whether ARE-mediated mRNA decay is altered by the expression of HSPB3

We were able to show the subcellular localization of HSPB3 and HSPB3(R7S). Our preliminary results confirmed that HSPB1 is a cytoplasmic protein and showed that HSPB3 and HSPB3(R7S) are nuclear proteins; however, HSPB3 and HSPB3(R7S) are not localized in the nucleolus. Since both HSPB3 and HSPB3(R7S) were found to be localized in the nucleus but not the nucleolus, we preliminarily concluded that the R7S mutation does not have a significant effect on the subcellular localization of HSPB3. The

localization of the proteins was visibly clear in the cells; however, we only conducted one trial. More trials must be conducted to confirm our results.

Our subsequent experiments with HSPB3 and HSPB3(R7S) were unsuccessful. Transfected HSB3 and HSPB3(R7S) have proven difficult to express via chemical transfection with the FuGENE HD transfection reagent (Roche) or a Qiagen kit. Therefore, we are currently developing a lenti-viral transfection vector to transfect the HSPB3 and HSPB3(R7S) genes. If this is not successful, other transfection mechanisms must be tried to determine how best to transfect exogenous HSPB3 and HSPB3(R7S) genes into macrophages or some other cell type that endogenously expresses TNFα.

Future Directions

To determine if HSPB1(R136W) has an inhibitory affect on ARE-mediated mRNA decay *in vitro*, the mRNA decay assay described in Aim 1 must be repeated. Currently, we are studying the effect of HSPB1(R136W) on ARE-mediated mRNA decay of an endogenously expressed ARE-containing mRNA. Therefore, we also aim to determine if HSPB1(R136W) affects ARE-mediated mRNA decay of an exogenous ARE-containing mRNA. To study this, we will double transfect the macrophages with an HSPB1 (mutant or wild-type) gene and a β-globin gene (mutant or wild-type). The mutant β-globin will contain the TNFα ARE, but the wild-type β-globin will not contain an ARE on its mRNA. We will then perform the mRNA decay assay described in Aim 1 on the β-globin mRNA.

To study the affect of HSPB1(R136W) on ARE-mediated mRNA decay *in vivo*, we must directly measure the rate of mRNA decay from tissue samples of HSPB1 and HSPB1(R136W) transgenic mice. We can do this by isolating RNA directly from tissue samples of these mice or using laser-capture micro-dissection to isolate specific cell types from which the RNA can be extracted. We will then convert the RNA to cDNA and quantitate the levels of mRNA via QPCR as described above. We can use these techniques to measure the steady state of ARE-mediated mRNA decay in the mice, or we can stress the mice with an injection of LPS, and then measure the rate of ARE-mediated mRNA decay in response to cell stress. We will be able to compare ARE-mediated mRNA decay in the PrP-HSPB1(R136W) mice to ARE-mediated mRNA decay in both PrP-HSPB1 mice and non-transgenic control mice. In addition, it is necessary to develop a transgenic mouse expressing HSPB1(R136W) that develops a clinical neuropathy. To do so, we are currently developing two BACs with HSPB1(R136W) or wild-type HSPB1 that we will use to develop transgenic mice that ubiquitously express HSPB1(R136W) or wild-type HSPB1. We will then directly measure the rate of ARE-mediated mRNA decay in these mice by the previously-stated techniques.

We must also determine how HSPB3 and HSPB3(R7S) affect ARE-mediated mRNA decay. To do so, we need to develop a successful transfection paradigm to express HSPB3 or HSPB3(R7S) either by a lenti-viral vector or another method for transfection. We will then perform the mRNA decay assay as described above in those transfected macrophages. It is also necessary to develop a transgenic mouse expressing

HSPB3 or HSPB3(R7S) to determine the affect of HSPB3 and HSPB3(R7S) on ARE-mediated mRNA decay *in vivo*.

We believe that mRNA processing may be part of the common mechanism of all MNDs. Therefore, in addition to repeating the mRNA decay assay in models of dHMN and ALS, we must determine the effectiveness of ARE-mediated mRNA decay in models of other MNDs.

Lastly, we would also like to determine whether the alpha-crystallin domain is particularly susceptible to mutation, what function the alpha-crystallin serves, and whether mutations in among the different sHSP domains affect different sHSP functions.

Significance

There are no effective therapies for MNDs. Mutations in sHSPs are linked to MNDs; specifically, mutations in HSPB1, HSPB3, and HSPB8 are known to cause dHMN [5-6, 9]. We believe that mutations in HSPB1, HSPB3, and HSPB8 all lead to the same functional consequences and act by a common mechanism to cause dHMN, and that this mechanism is common to MNDs in general. Determining whether the mutations in HSPB1 and HSPB3 alter ARE-mediated mRNA decay *in vitro* and *in vivo* will help to uncover the mechanism of dHMN. If the mutations in HSPB1 and HSPB3 have a harmful effect on ARE-mediated mRNA decay, then ARE-mediated mRNA decay may be part of the common mechanism of sHPS mutations leading to dHMN.

In addition, we believe that a common pathway is affected in all MNDs. We hypothesize that mRNA processing may be part of the common pathway. Therefore,

studying ARE-mediated mRNA decay in a model ALS in addition to models of dHMN will help us determine if ARE-mediated mRNA decay is altered in models of both diseases, and therefore, if ARE-mediated mRNA decay is potentially part of the common mechanism of MNDs in general. The knowledge of the mechanism of dHMN and MNDs will lead to new treatments for dHMN and MNDs that will extend and improve the quality of life of those living with these diseases.

References

1. Mitchell JD, Borasio GD. Amyotrophic lateral sclerosis. *Lancet* 2007 Jun 16;369(9578):2031-41.
2. Rothstein JD. Current hypotheses for the underlying biology of amyotrophic lateral sclerosis. *Ann Neurol* 2009 Jan;65(S1):S3-S9.
3. Kolb SJ, Sutton S, Schoenberg DR. RNA processing defects associated with diseases of the motor neuron. *Muscle Nerve*. 2010 Jan;41(1):5-17.
4. Reilly MM. Classification and diagnosis of the inherited neuorpathies. *Ann Indian Acad Neurol.*2009 (Apr-Jun; 12(2): 80-88.
5. Irobi J, De Jonghe P, Timmerman V. Molecular genetics of distal hereditary motor neuropathies. *Hum Mol Genet* 2004 Oct 1;13(2):R195-R202.
6. Irobi J, Van Impe K, Seeman P, Jordanova A, Dierick I, et al. Hot-spot residue in small heat-shock protein 22 causes distal motor neuropathy. *Nat Genet*. 2004 Jun;36(6):597-601.
7. Evgrafov OV, Mersiyanova I, Irobi J, Van Den Bosch L, Dierick I, et al. Mutant small heat-shock protein 27 causes axonal Charcot-Marie-Tooth disease and distal hereditary motor neuropathy. *Nat Genet.* 2004 Jun;36(6):602-6.
8. Fontaine JM, Sun X, Hoppe AD, Simon S, Vicart P, Welsh MJ, Benndorf R. Abnormal small heat shock protein interactions involving neuropathy-associated HSP22 (HSPB8) mutants. *FASEB J*. 2006 Oct;20(12):2168-70. Epub 2006 Aug 25.
9. Kolb SJ, Snyder PJ, Poi EJ, Renard EA, Bartlett A, et al. Mutant small heat shock protein B3 causes motor neuropathy: utility of a candidate gene approach. *Neurology*. 2010 Feb 9;74(6):502-6.
10. Kappé G, Franck E, Verschuure P, Boelens WC, Leunissen JAM, de Jong WW. The human genome encodes 10 α-crystallin–related small heat shock proteins: HspB1–10. *Cell Stress Chaperones*. 2003 Jan 2003 [cited 30 Nov 2009];8(1):53-61.
11. Boelens WC, Croes Y, de Ruwe M, de Reu L, de Jong WW. Negative charges in the C-terminal domain stabilize the aB-crystallin complex. *J Biol Chem* 1998 Oct 23;273:28085-28090.
12. Welsh MJ, Gaestel M. Small heat-shock protein family: Function in health and disease. *Ann N Y Acad Sci.* 1998;851:28-35.
13. Rogalla T, Ehrnsperger M, Preville X, Kotlyarov A, Lutsch G, Ducasse C, et al. Regulation of Hsp27 oligomerization, chaperone function, and protective activity against oxidative stress/tumor necrosis factor alpha by phosphorylation. *J Biol Chem* 1999 Jul 2;274(27):18947-18956.
14. Sinsimer KS, Gratacós FM, Knapinska AM, Lu J, Krause CD, Wierzbowski AV, et al. Chaperone Hsp27, a novel subunit of AUF1 protein complexes, functions in AU-rich element-mediated mRNA decay. *Mol Cell Biol* 2008 Sep;28(17):5223-5237.
15. Akbar MT, Lundberg AM, Liu K, Vidyadaran S, Wells KE, Dolatshad H, et al. The neuroprotective effects of heat shock protein 27 overexpression in transgenic animals

against kainate-induced seizures and hippocampal cell death. J Biol Chem 2003 May 30;278(22):19956-19965.
16. Borchelt, D. R., J. Davis, et al. (1996). "A vector for expressing foreign genes in the brains and hearts of transgenic mice." Genet Anal 13(6): 159-163.
17. Xia, R. H., N. Yosef, et al. (2010). "Dorsal caudal tail and sciatic motor nerve conduction studies in adult mice: Technical aspects and normative data." Muscle Nerve.
18. Yuan Y, Shen H, Yao J, Hu N, Ding F, Gu X. The protective effects of Achyranthes bidentata polypeptides in an experimental model of mouse sciatic nerve crush injury. Brain Res Bull. 2010 Jan 15;81(1):25-32.
19. Butchbach, M. E., J. D. Edwards, et al. (2007). "Abnormal motor phenotype in the SMNDelta7 mouse model of spinal muscular atrophy." Neurobiol Dis 27(2): 207-219.
20. Dziennis S, Van Etten RA, Pahl HL, Morris DL, Rothstein TL, Blosch CM, Perlmutter RM, Tenen DG. The CD11b promoter directs high-level expression of reporter genes in macrophages in transgenic mice. Blood. 1995 Jan 15;85(2):319-29.
21. Friedman MJ, Li S, Li XJ. Activation of Gene Transcription by Heat Shock Protein 27 May Contribute to Its Neuronal Protection. *J Biol Chem*. 2009 Oct 9; 284(41):27944-51. Epub 2009 Aug 5.
22. Gurney ME, Pu H, Chiu AY, Dal Canto MC, Polchow CY, Alexander DD, Caliendo J, Hentati A, Kwon YW, Deng HX, et al. Motor neuron degeneration in mice that express a human Cu,Zn superoxide dismutase mutation. *Science*. 1994 Jun 17;264(5166):1772-5. Erratum in *Science* 1995 Jul 14;269(5221):149.
23. Acevedo-Arozena A, Kalmar B, Essa S, Ricketts T, Joyce P, Kent R, Rowe C, Parker A, Gray A, Hafezparast M, Thorpe JR, Greensmith L, Fisher EM. A comprehensive assessment of the SOD1G93A low-copy transgenic mouse, which models human amyotrophic lateral sclerosis. Dis Model Mech. 2011 May 2. [Epub ahead of print]
24. Clement AM, Nguyen MD, Roberts EA, Garcia ML, Boillée S, Rule M, McMahon AP, Doucette W, Siwek D, Ferrante RJ, Brown RH Jr, Julien JP, Goldstein LS, Cleveland DW. Wild-type nonneuronal cells extend survival of SOD1 mutant motor neurons in ALS mice. *Science*. 2003 Oct 3;302(5642):113-7. Erratum in *Science*. 2003 Oct 24;302(5645):568.
25. Di Giorgio, F. P., M. A. Carrasco, et al. (2007). "Non-cell autonomous effect of glia on motor neurons in an embryonic stem cell-based ALS model." Nat Neurosci 10(5): 608-614.
26. Nagai, M., D. B. Re, et al. (2007). "Astrocytes expressing ALS-linked mutated SOD1 release factors selectively toxic to motor neurons." Nat Neurosci 10(5): 615-622.